

Corrosion Inhibition of Mild Steel in Hydrochloric Acid using 4-(pyridin-2yl)-N-p-tolylpiperazine-1-carboxamide

Sumathi Paramasivam^{1,*}, Kannan Kulanthai², Gnanavel Sadhasivam², Rekha Subramani¹

¹Department of Chemistry, Knowledge Institute of Technology, Salem, Tamilnadu, India.

²Department of Chemistry, Government College of Engineering, Salem, Tamilnadu, India

*E-mail: sumathi.murugan25@gmail.com

Received: 8 July 2015 / Accepted: 16 February 2016 / Published: 1 April 2016

4-(pyridin-2yl)-N-p-tolylpiperazine-1-carboxamide(PTC) was synthesized and characterized using FT-IR, ¹H NMR, and ¹³C NMR spectra. The inhibitive action of 4-(pyridin-2yl)-N-p-tolylpiperazine-1-carboxamide(PTC) against corrosion of mild steel in a 1M HCl solution was investigated using weight loss measurements, potentiodynamic polarization and electrochemical impedance spectroscopy(EIS). The inhibition efficiency increases with increasing concentration of inhibitor whereas it decreases with increasing temperature. EIS results showed that the change in the impedance parameters (Rct and Cdl) with concentration of (PTC) is indicative of the adsorption of molecules leading to the formation of a protective layer on the surface of mild steel. Potentiodynamic polarization study showed that PTC is a mixed type inhibitor. Surface analysis by SEM confirmed the formation of adsorbed protective layer of the inhibitor on the steel surface. The adsorption of inhibitor follows the Langmuir adsorption isotherms. Thermodynamic parameters such as activation energy (Ea), free energy change (ΔG_{ads}), enthalpy change (ΔH_{ads}) and entropy change (ΔS_{ads}) were also calculated and discussed in detail.

Keywords: Corrosion; Inhibition efficiency; HCl, Mild steel, Weight loss, EIS, Tafel Polarization and adsorption.

1. INTRODUCTION

Mild steel is widely applied as the constructional materials in many industries due to its excellent mechanical properties and low cost [1]. Hydrochloric acid solutions are widely used in several industrial processes. Some of the important fields of application being acid pickling of steel, chemical cleaning and processing, ore production and pipelines, other corrosion products from the surface of equipment's such as heat exchangers, boilers, cooling towers, etc. [2-3] Because of the general aggression of acid solutions, inhibitors are commonly used to reduce the corrosive attack on metallic materials. The use of corrosion inhibitors constitutes one of the most economical

ways to mitigate the corrosion rate, preserve industrial facilities and protect metal surfaces against corrosion in acidic media. Inhibitors are effective in reducing the dissolution rate of metals. Corrosion inhibitors are of considerable practical importance because they are extensively employed in both reducing metallic wastes during production and minimizing the risk of material failure [4]. Use of inhibitor is one of the most effective strategies to improve the corrosion resistance of metal, compared with other corrosion protection technologies.

Especially some of the newly synthesized organic compounds are used as the inhibitors for the mild steel corrosion [5-7]. Many studies have reported the application of organic inhibitors, Most effective inhibitors are organic compounds containing electronegative functional groups and π electrons in triple or conjugated double bonds[8-13] which are usually heterocyclic compounds containing heteroatoms such as Oxygen, Nitrogen, Sulfur, etc., for protecting metals against acidic corrosion[14-15]. The inhibition efficiency should increase in the order $O < N < S < P$ [16]. The effect of inhibitors adsorbed on metallic surfaces in acid solutions, is to slow down the cathodic reaction as well as the anodic process of dissolution of the metal.

In case of corrosion in an acid medium, the corrosion rate increases with temperature because the hydrogen evolution over potential decreases [17]. Temperature dependence of the inhibitor efficiency (IE) and the comparison of the values of effective activation energy (E_a) of the corrosion process both in the absence and in the presence of inhibitors lead to some conclusions concerning the mechanism of the inhibiting action and type of adsorption. In many cases, the efficiency of an organic compound as an inhibitor is due to its adsorption on the metal surface forming a barrier layer which separates the metal from the corrosive media [18].

The present investigation reports the use of newly synthesized 4-(pyridin-2yl)-N-p-tolylpiperazine-1-carboxamide(PTC) as a corrosion inhibitor for mild steel corrosion in 1M HCl.

2. EXPERIMENTAL

2.1 Preparation of Specimens

Mild steel specimens of composition Fe = 99.686, Ni = 0.012, Mo = 0.016, Cr = 0.042, S = 0.015, Si = 0.007, Mn = 0.196, and C = 0.017 were cut to size of 5 cm \times 1.5 cm. The surface of specimens were polished with emery papers ranging from 110 to 410 grades and degreased with trichloroethylene, washed with double distilled water, and finally dried. Dried specimens were stored in vacuum desiccators containing silica gel. Weight loss measurements were performed as per ASTM method described previously (28).

2.2 Preparation of Test Solutions

1M HCl solution was prepared by adding 83.3 ml of 12N AR-Grade HCl in 1,000ml of double distilled water.

2.7 Weight loss studies

Weight loss measurements were carried out by weighing the mild steel specimens before and after immersion in the glass vessel containing 100 ml test solution. A clean weighed mild steel specimen was completely immersed in the solution by hanging from the glass rod using Teflon thread for different time intervals (1 hr, 2 hr, 3 hr and 4 hr) with and without inhibitor at 303K. The same procedure was repeated for different temperatures (303 K, 313 K, 323 K and 333K) with one hr immersion period. From the weight loss measurements, corrosion rate, inhibition efficiency and surface coverage were calculated using the following equations (1), (2), and (3)

2.7.1 Corrosion Rate

$$CR = \frac{8.76 \times 10,000W}{ATD} \quad (1)$$

Where T= time of exposure in hrs; W= weight loss of test specimen in g; A= area of test specimen in cm², D=density of material in gcm⁻³, CR=corrosion rate in mmpy,

2.7.2 Inhibition Efficiency

$$IE\% = \frac{W_b - W_{Inh}}{W_b} \times 100 \quad (2)$$

2.7.3 Surface coverage

$$\Theta = \frac{W_b - W_{Inh}}{W_b} \quad (3)$$

where W_b and $W_{(Inh)}$ are the corrosion rates of mild in the absence and presence of the inhibitor in 1M HCl respectively at the same temperature.

2.8 Potentiodynamic polarization studies

The corrosion cell used had three electrodes. The reference electrode was a saturated calomel electrode (SCE). A platinum electrode was used as counter electrode. Mild steel (MS) with exposed area of 1cm² was used as working electrode. All potentials given in this study were referred to this reference electrode. All the three electrodes were immersed in 100 ml of 1M HCl solution. The electrochemical behavior of mild steel in inhibited and uninhibited solution was studied by recording anodic and cathodic potentiodynamic polarization curves. The polarization measurements were carried out at a scan rate of 0.2 mV/s using Electrochemical analyzer Model CHI608D instrument. The corrosion parameters such as corrosion potential (E_{corr}), corrosion current (I_{corr}) cathodic Tafel slope (b_c), and anodic Tafel slope (b_a) were obtained.

2.9 AC Impedance study

AC impedance measurements were carried out in the corrosion potential frequency range of 10 kHz to 0.01kHz from the open circuit potential using Electrochemical analyzer (Model CHI608D(E)). The solution resistance (R_s) and total resistance(R_t) were obtained from the low frequency and high frequency intercepts on Z' -axis of Nyquist plot, respectively. The difference between R_t and R_s values give the charge transfer resistance R_{ct} value.

2.10 Surface Analysis

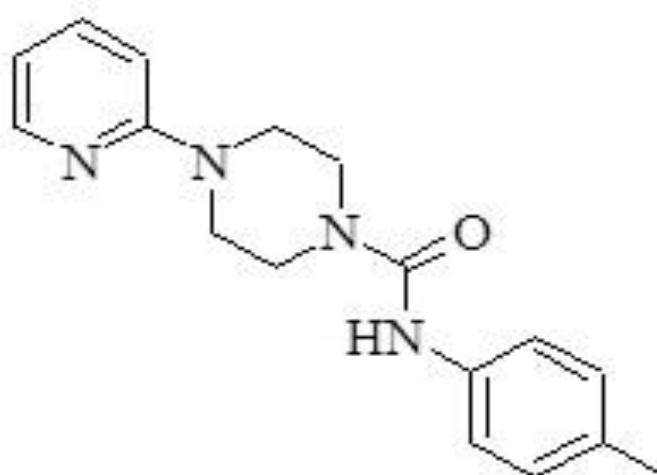
2.10.1 FT-IR and scanning Electron Microscope (SEM) Analysis

The mild steel specimens were immersed for 1 hr in 1M HCl solution with and without inhibitor. These specimens were cleaned with double distilled water and dried at room temperature. The transmittance and reflectance of the infrared rays at different frequencies were translated into an IR absorption plot consisting of reverse peaks. The morphology of treated mild steel surface was examined by using scanning electron microscope.

3. RESULTS AND DISCUSSION

3.1 Characterization of 4-(pyridin-2yl)-N-p-tolylpiperazine-1-carboxamide(PTC)

Newly synthesized 4-(pyridin-2yl)-N-p-tolylpiperazine-1-carboxamide was characterized using the data obtained from the FT-IR and NMR spectra.



Molecular weight: 296, melting point: 170-171°C

Figure 1. Structure of 4-(pyridin-2yl)-N-p-tolylpiperazine-1-carboxamide(PTC)

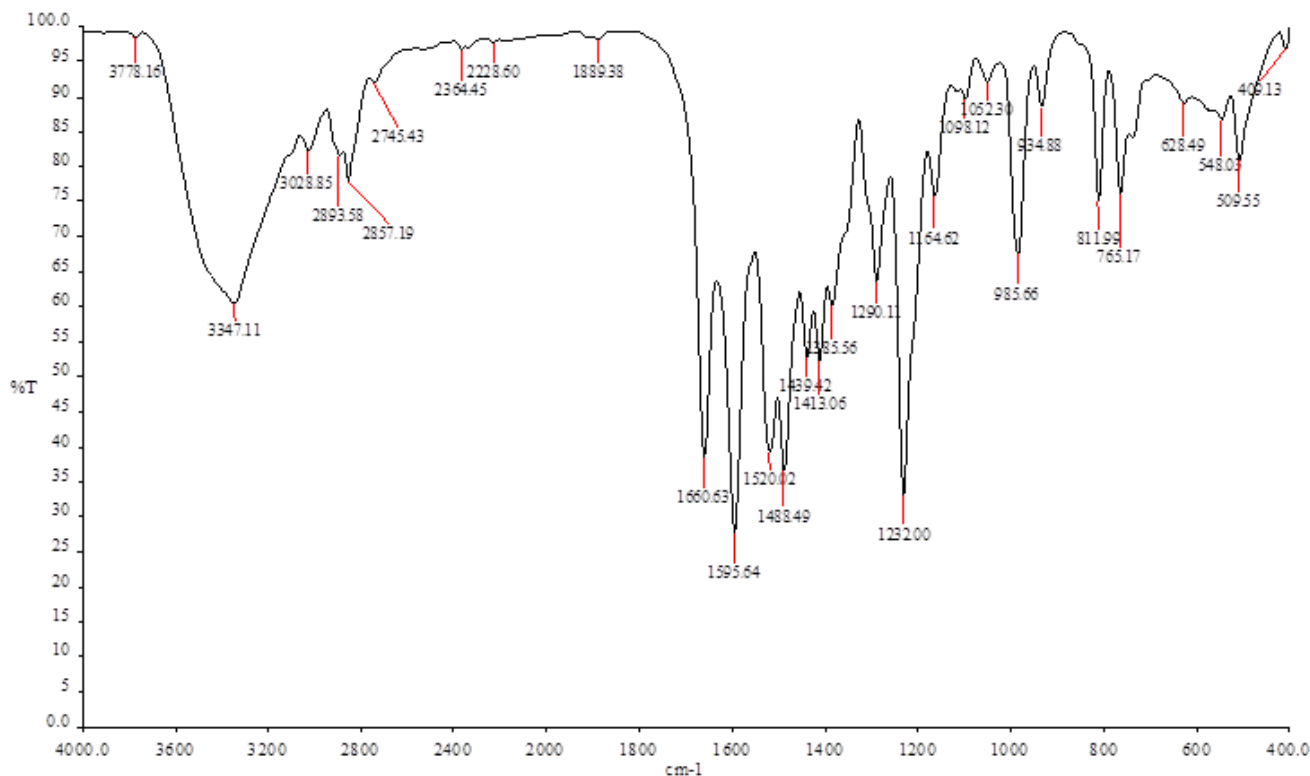


Figure 2. FT-IR Spectrum of 4-(pyridin-2yl)-N-p-tolylpiperazine-1-carboxamide(PTC)

Table 1. FT-IR spectral data of 4-(pyridin-2yl)-N-p-tolylpiperazine-1-carboxamide

Peak value (cm ⁻¹)	Possible groups	Peak value (cm ⁻¹)	Possible groups
3778.16	2 ⁰ Amine	2857.19	C-H symmetric stretch
3347.11	OH (H bonded)	1660.63	C=C attached to aromatic ring
3028.85	C-H group in the aromatic ring	1595.64	C=O attached to amine group

3.1.1 FT-IR spectral Analysis of 4-(pyridin-2yl)-N-p-tolylpiperazine-1-carboxamide

The FT-IR spectral data of PTC are given in Table.1 and the spectrum recorded is shown in Fig.2. The peaks appeared in various regions of FT-IR spectrum of the functional groups present in the inhibitor are represented as follows. A sharp peak appeared at 3778.16 cm⁻¹ is 2⁰ amine group, the peak at 3347.11cm⁻¹ is due to the OH (H-bonded) and the sharp peak appeared in the region of 3028.85 cm⁻¹ is attributed to the C-H group in the aromatic ring . The peak appeared in the region of 2857.19cm⁻¹ is due to C-H symmetric stretch. The peak appeared at 1660.63 cm⁻¹ and 1595.64 cm⁻¹ are attributed to the C=C attached to aromatic ring and C=O attached to amine group in the structure. It is

conformed from the table that the compound contains amine, nitrogen and aromatic ring as shown in fig1.

3.1.2.1 NMR spectral analysis

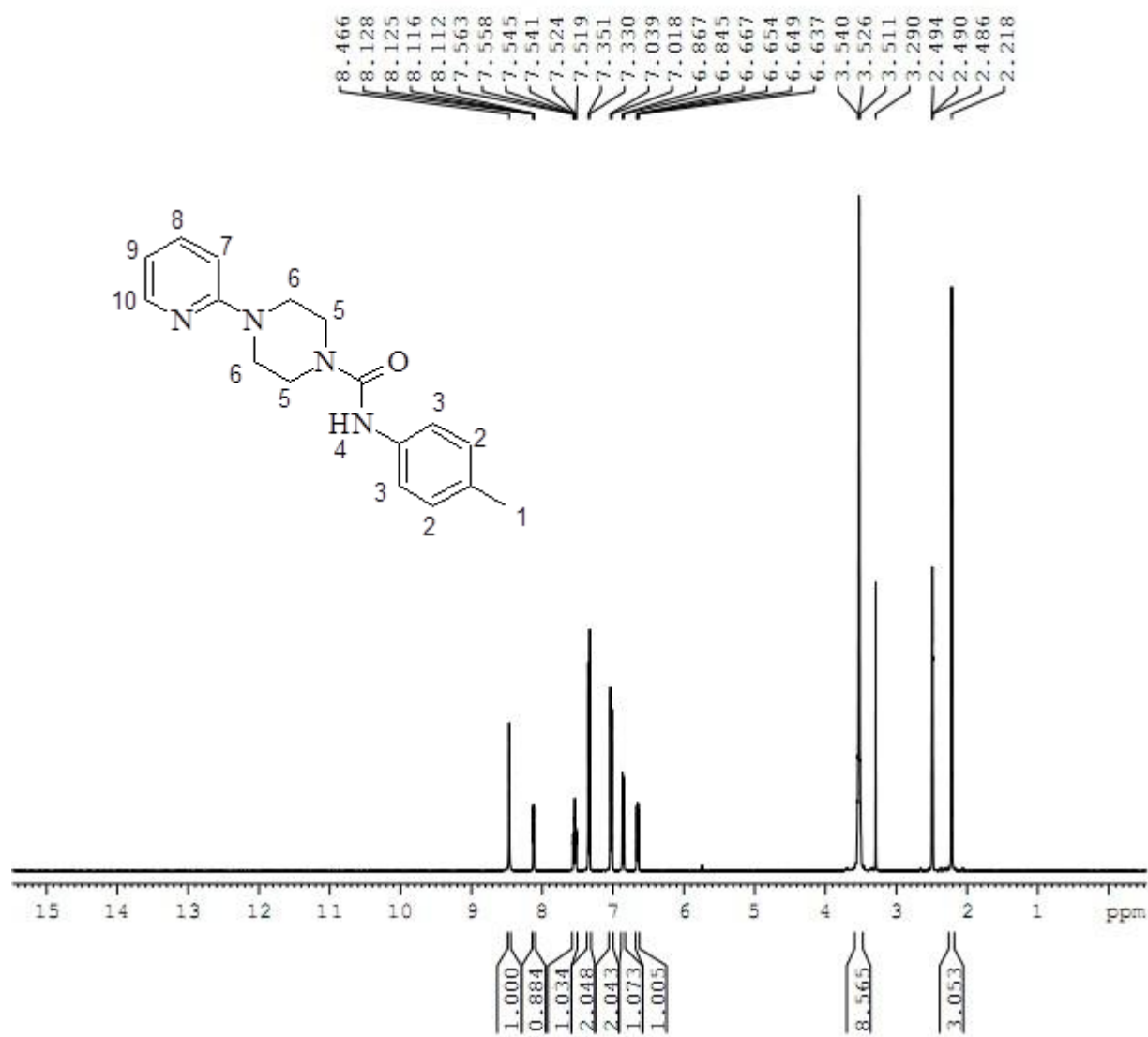


Figure 3. ^1H NMR spectrum of 4-(pyridin-2-yl)-N-p-tolylpiperazine-1-carboxamide

The structure was confirmed by ^1H NMR [200 MHz, DMSO]. The ^1H NMR spectral data of 4-(pyridin-2-yl)-N-p-tolylpiperazine-1-carboxamide are given in table 2. The recorded spectrum is shown in fig(3) The singlet at 2.21 ppm is assigned to three hydrogen atoms labeled as 1, Triplet at 3.51-3.54 ppm is assigned to eight hydrogen atoms numbered as 5,6, triplet 6.65 ppm is attributed to one hydrogen marked as 9, doublet at 6.94 ppm is assigned to one hydrogen atom labeled as 7, both doubled at 7.03 and 7.34 ppm are assigned to two hydrogen atoms numbered as 2,3. Triplet of doublet at 7.54 ppm is attributed to one hydrogen labeled as 8, doublet of doublet at 8.12 ppm is assigned to one hydrogen numbered as 10 and singlet at 8.46 ppm is attributed to one hydrogen labeled as 4.

Table 2. ^1H NMR data of 4-(pyridin-2yl)-N-p-tolylpiperazine-1-carboxamide

Sl.No	Chemical shift value δ	Splitting pattern	No. of a hydrogen	Proton numbered
1	2.21	Singlet	3	1
2	3.51-3.54	Triplet	8	5,6
3	6.65	Triplet	1	9
4	6.94	Doublet	1	7
5	7.03	Doublet	2	2
6	7.34	Doublet	2	3
7	7.54	Triplet of doublet	1	8
8	8.12	Doublet of doublet	1	10
9	8.46	Singlet	1	4

3.1.2.2 ^{13}C NMR analysis of 4-(pyridin-2yl)-N-p-tolylpiperazine-1-carboxamide.

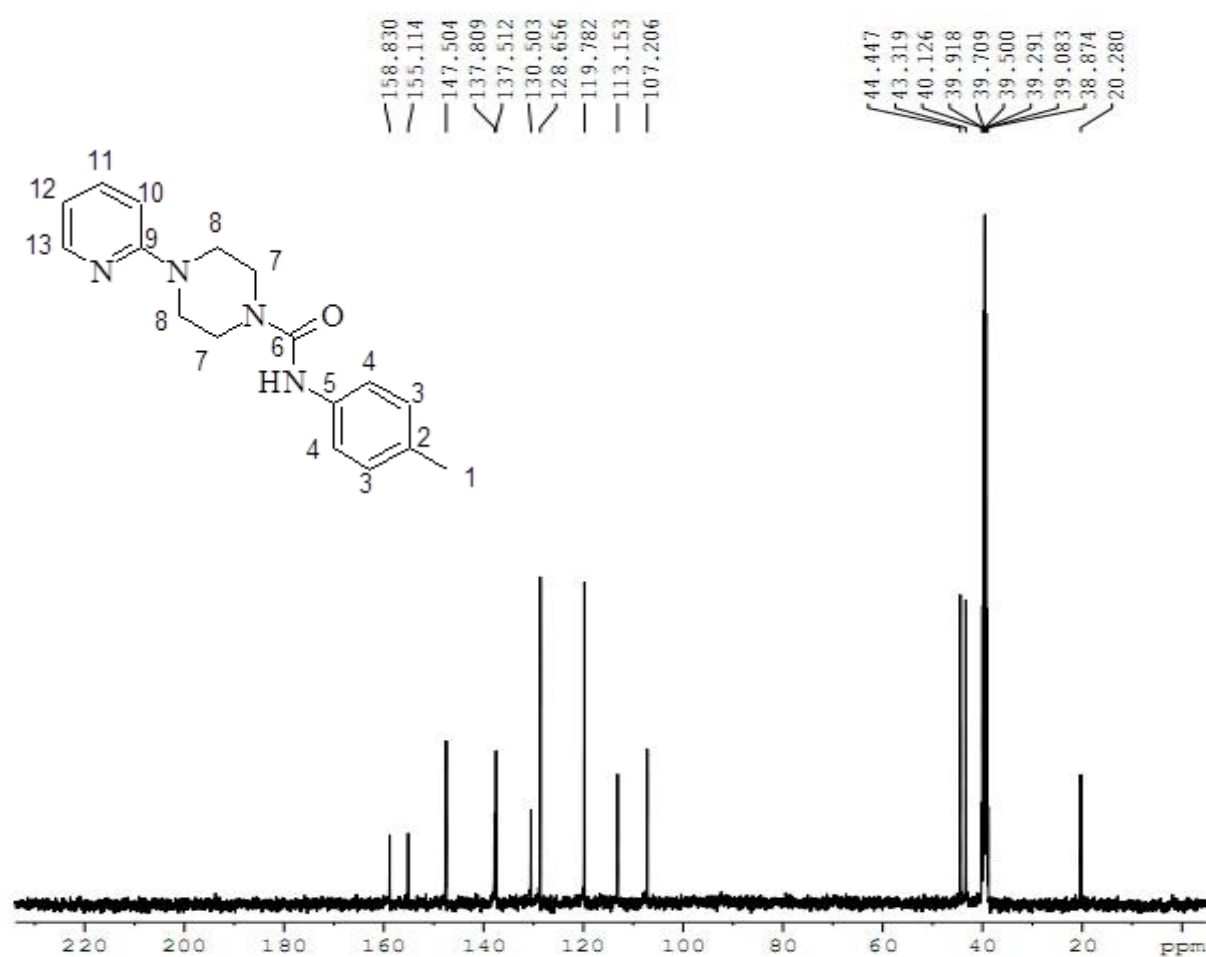
**Figure 4.** ^{13}C NMR spectrum of 4-(pyridin-2yl)-N-p-tolylpiperazine-1-carboxamide

Table 3. ^{13}C NMR data of 4-(pyridin-2yl)-N-p-tolylpiperazine-1-carboxamide

Sl.No	Chemical shift value δ	Splitting pattern	Number of carbon	Carbon numbered in structure
1	20.2	Singlet	1	1
2	43.3	Singlet	2	7
3	44.4	Singlet	2	8
4	107.2	Singlet	1	10
5	113.1	Singlet	1	12
6	119.7	Singlet	1	4
7	128.6	Singlet	1	3
8	130.5	Singlet	1	2
9	137.5	Singlet	1	5
10	137.8	Singlet	1	11
11	147.5	Singlet	1	13
12	155.1	Singlet	1	9
13	158.8	Singlet	1	6

The ^{13}C NMR spectral data of 4-(pyridin-2yl)-N-p-tolylpiperazine-1-carboxamide are presented in table 3. The recorded spectrum of synthesized compound is shown in fig(4). The singlet at 20.2 ppm is assigned to one carbon labeled as 1, singlet at 43.3 ppm is attributed to two carbon position in structure numbered as 7, singlet at 44.4 ppm is assigned to two carbon labeled as 8, singlet at 107.2 ppm is attributed to one carbon labeled as 10, singlet at 113.1 ppm is referred to one carbon position in structure number 12, singlet at 119.7, 128.6 and 130.5 ppm are assigned to one carbon various positions in structure numbered as 4, 3 and 2. Singlet at 137.5, 137.8, 147.5 and 155.1 ppm are attributed to one carbon of various positions in structure labeled as 5, 11, 13 and 9. Singlet at 158.8 is assigned to one carbon labeled as 6.

3.2 Corrosion studies

3.2.1 Weigh loss method

The inhibition efficiency of the inhibitor on the mild steel in 1M HCl with increasing concentration was studied by weight loss measurements. The values of corrosion rate (CR), surface coverage (Θ) and corrosion inhibition efficiency (IE%) obtained from weight loss measurements for the mild steel specimens immersed in 1M HCl solution in the presence of different concentrations (0.00-1200ppm) of inhibitor (PTC) for various immersion periods of 1hr, 2hrs and 3hrs at constant temperature (303K) are listed in Table 4. The inhibition efficiency (IE%) increased with respect to time and concentration of the inhibitor. The maximum inhibition efficiency of 4-(pyridin-2yl)-N-p-tolylpiperazine-1-carboxamide inhibitor was found to be 98.47 % in 1M HCl for 900 ppm inhibitor concentration at 3hrs.

Table 4. Corrosion parameters obtained from Weight loss Measurements at 303K (1hr, 2hr and 3hr)

conc (ppm)	1hr			2hr			3hr		
	CR	(Θ)	IE%	CR	(Θ)	IE%	CR	(Θ)	IE%
Blank	139.3	-	-	285.6	-	-	318.5	-	-
100	19.3	0.8616	86.16	32.5	0.8862	88.62	31.3	0.9017	90.17
300	9.5	0.9316	93.16	14.9	0.9479	94.79	16.4	0.9486	94.86
500	7.4	0.9466	94.66	12.9	0.9547	95.47	13.4	0.958	95.8
700	4.8	0.9658	96.58	8.2	0.9713	97.13	7.7	0.9757	97.57
900	3.4	0.9754	97.54	5.6	0.9805	98.05	4.9	0.9847	98.47
1100	8.3	0.9402	94.02	16.1	0.9435	94.35	23.4	0.9265	92.65
1200	11.3	0.9188	91.88	26.0	0.9088	90.88	26.6	0.9164	91.64

Table 5. Corrosion parameters obtained from weight loss measurements at different temperatures (303 to 333K) for 1hr.

conc (ppm)	303K			313K			323K			333K		
	CR	(Θ)	IE%	CR	(Θ)	IE%	CR	(Θ)	IE%	CR	(Θ)	IE%
Blank	139.3			761.5			1410.5			1618.1		
100	19.3	0.8616	86.16	177.7	0.767	76.67	450.7	0.6805	68.05	748.7	0.5373	53.73
300	9.5	0.9316	93.16	78.4	0.897	89.7	243.0	0.8277	82.77	383.6	0.7629	76.29
500	7.4	0.9466	94.66	40.8	0.947	94.65	143.1	0.8985	89.85	294.6	0.8179	81.79
700	4.8	0.9658	96.58	31.2	0.959	95.9	121.1	0.9141	91.41	153.3	0.9053	90.53
900	3.4	0.9754	97.54	20.8	0.973	97.26	72.5	0.9486	94.86	135.4	0.9163	91.63
1100	8.3	0.9402	94.02	83.9	0.89	88.98	313.1	0.7781	77.81	445.2	0.7249	72.49
1200	11.3	0.9188	91.88	113.7	0.851	85.07	417.2	0.7042	70.42	551.7	0.659	65.9

Table 5 shows the change in the value of inhibition efficiency, surface coverage and corrosion rate for the various concentration of the inhibitor in 1M HCl for a period of 1hr at various temperatures. The inhibition efficiency was found to increase with increasing concentration of inhibitor and while it decreased with increasing temperature shown in fig (5). This can be attributed to the desorption of some adsorbed inhibitor molecules on the metal surface with increase in temperature leading to decrease in inhibition efficiency [19]. The maximum inhibition efficiency was found to be 97.54% in 1 M HCl for 900 ppm PTC at 303K.

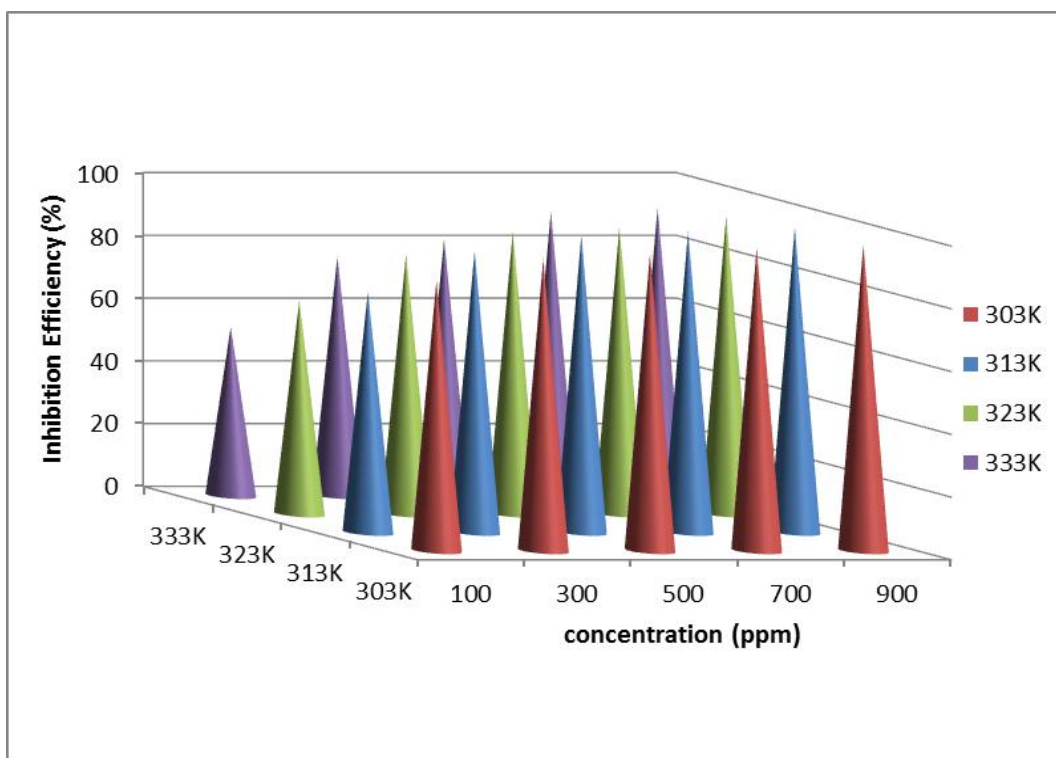


Figure 5. Corrosion parameters obtained from weight loss measurements at different temperatures (303 to 333K) for 1hr.

3.2.1.1 Thermodynamic and activation parameters

Table 6 shows the computed values of activation energy (E_a), enthalpy of activation (ΔH), entropy of activation (ΔS) and free energy of adsorption (ΔG_{ads}). The evident activation energy (E_a) for dissolution of mild steel in 1M HCl solution was ascertained by using the Arrhenius equation:

$$\text{LogCR} = \frac{-E_a}{2.303RT} + \log A \quad (4)$$

where R is the global gas constant ($8.314 \text{ JK}^{-1}\text{mol}^{-1}$), T is the absolute temperature (K) and A is the Arrhenius pre-exponential factor. Fig 6. demonstrates the Arrhenius plots of log CR is taken across y-axis and 1/T is taken down x-axis for the corrosion for degeneration of mild steel in a 1M HCl solution in the presence of inhibitors at concentration ranging from 0.00 to 1200ppm.

From Fig 6, the slope of each discrete line was determined, and the activation energy was calibrated by using the expression $E_a = -\text{slope} \times 2.303R$. It could be seen that the E_a is directly proportional to inhibitors concentration. This shows decrease in dissolution rate of mild steel due to formation of barrier by adsorption of inhibitor on its surface [20].

The values of ΔH and ΔS were calculated by using the transition state equation

$$\text{CR} = \frac{RT}{Nh} \exp\left(\frac{\Delta S}{R}\right) \exp\left(-\frac{\Delta H}{RT}\right) \quad (5)$$

where, h is planck's constant and N is the Avogadro number, respectively.

A plot of $\log(\text{CR}/T)$ versus 1/T shown in fig (7) gave straight lines with a slope of $-\Delta H/2.303R$ and an intercept of $[\log(R/Nh) + (\Delta S/2.303R)]$, from which the activation thermodynamic parameters (ΔH and ΔS) were reckoned, and listed in table 6. The positive sign of enthalpy and

negative sign ΔS shows that mild steel dissolution process is endothermic and formation of activation rate resolving of inhibitors. Where dissociation step indicates the decline in disorder in which reactants gets converted to activated complex [21].

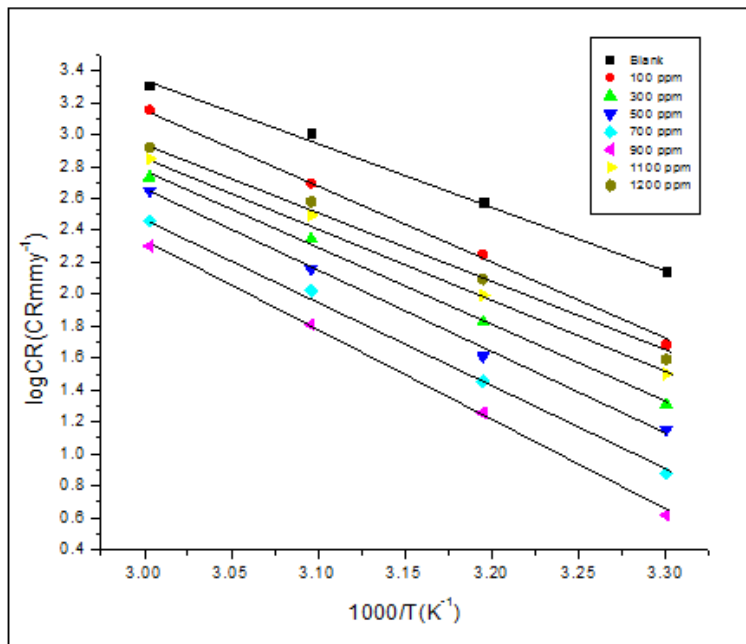


Figure 6. Arrhenius plots of log CR Vs 1000/T for mild steel corrosion 1M HCl containing with and without inhibitor (PTC).

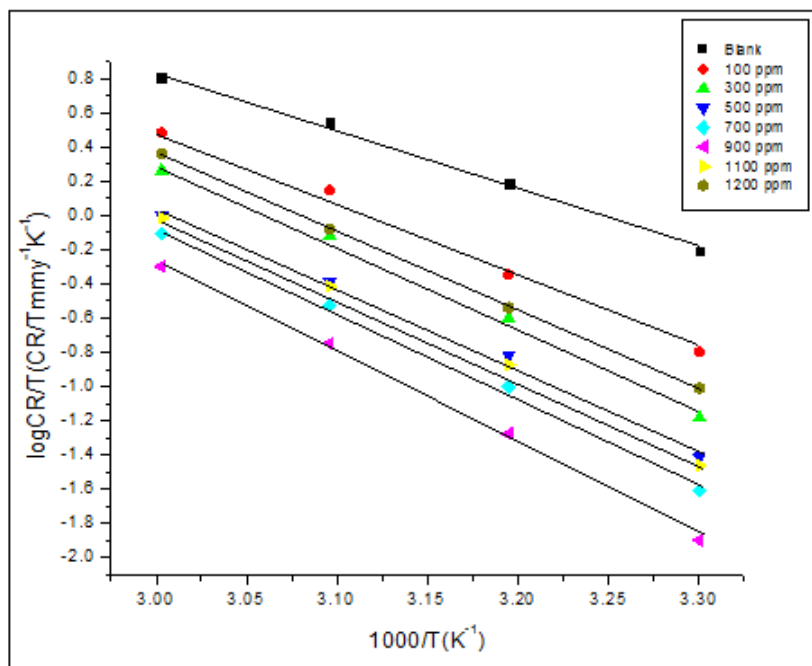


Figure 7. Transition state plots of log CR/T Vs 1000/T for mild steel corrosion 1M HCl containing with and without inhibitor(PTC).

It is observed from the Table 6 that E_a values are highly influenced in the presence of inhibitors rather than its absence of inhibitor. When E_a is higher the reaction is slow and very sensitive to temperature. The increase in the activation energy in the presence of inhibitors signifies physical adsorption [22]. The adsorption of (ΔG°_{ads}) calculated from surface coverage θ is listed in Table 7. The adsorption process becomes spontaneous and adsorbed layer of mild steel becomes stable when ΔG°_{ads} is negative the absolute ΔG°_{ads} value decrease because stability of adsorption layer is inversely proportional to temperature which there by confirms the physical adsorption.

$$\Delta G_{ads} = -RT \ln(55.5K) \quad (6)$$

$$K = \frac{\theta}{C(1-\theta)}$$

Table 6. Calculated values of activation energy (E_a), enthalpy (ΔH) and entropy (ΔS) for mild steel in 1M HCl with PTC

Concentration of PTC (ppm)	Activation Energy ($KJmol^{-1}$) (E_a)	Enthalpy ($KJmol^{-1}$) (ΔH)	Entropy ($Jmol^{-1}K^{-1}$) (ΔS)
Blank	67.7	96.5	-183.5
100	100.7	172.8	-177.4
300	104.9	187.6	-176.4
500	108.1	192.8	-176.1
700	112.0	198.8	-175.7
900	114.4	206.6	-175.2
1100	102.9	180.1	-177.0
1200	99.1	166.3	-178.0

Generally physisorption is electrostatic interaction between the charged molecules and the charged metal surfaces takes place. When ΔG° is less than $-40 KJ mol^{-1}$, chemisorption is charge sharing and transfer from organic molecules to the metal surface to form a coordinate type bond takes place when ΔG° is greater than $-40 KJ mol^{-1}$ [23-24].

Where Θ is the surface coverage on the metal surface, C is the concentration of inhibitor and K is the equilibrium constant. Based on the data presented in Table7 the value of the ΔG° was found to be less than $-40KJ mol^{-1}$. The negative value of ΔG_{ads} ranging from -18 to -26 KJ/mol indicated that the adsorption of inhibitor is spontaneous and also physically adsorbed on the mild steel in 1M HCl. The large values (ΔG°) and its negative sign are usually characteristic of strong interaction and a highly efficient adsorption. This confirms the occurrence of physical adsorption. A plot of C/Θ Vs C gives a straight line confirming that the adsorption of this compound on the metal surface obeys Langmuir adsorption isotherm (Fig.8)

Table 7. Calculated values of (ΔG_{ads}) for mild steel in 1 M HCl with PTC

concentration of PTC(ppm)	Values of (ΔG , kJ/mol)			
	303K	313K	323K	333K
100	-25.21	-24.91	-24.28	-23.57
300	-25.53	-25.23	-24.42	-24.06
500	-25.58	-25.45	-24.69	-24.28
700	-25.72	-25.53	-25.08	-24.41
900	-26.33	-26.01	-25.18	-24.73
1100	-21.63	-22.62	-20.08	-19.91
1200	-20.5	-21.57	-18.81	-18.02

3.2.1.2 Adsorption isotherm

Adsorption isotherms are very important in determining the mechanism of organic electrochemical reactions [25].

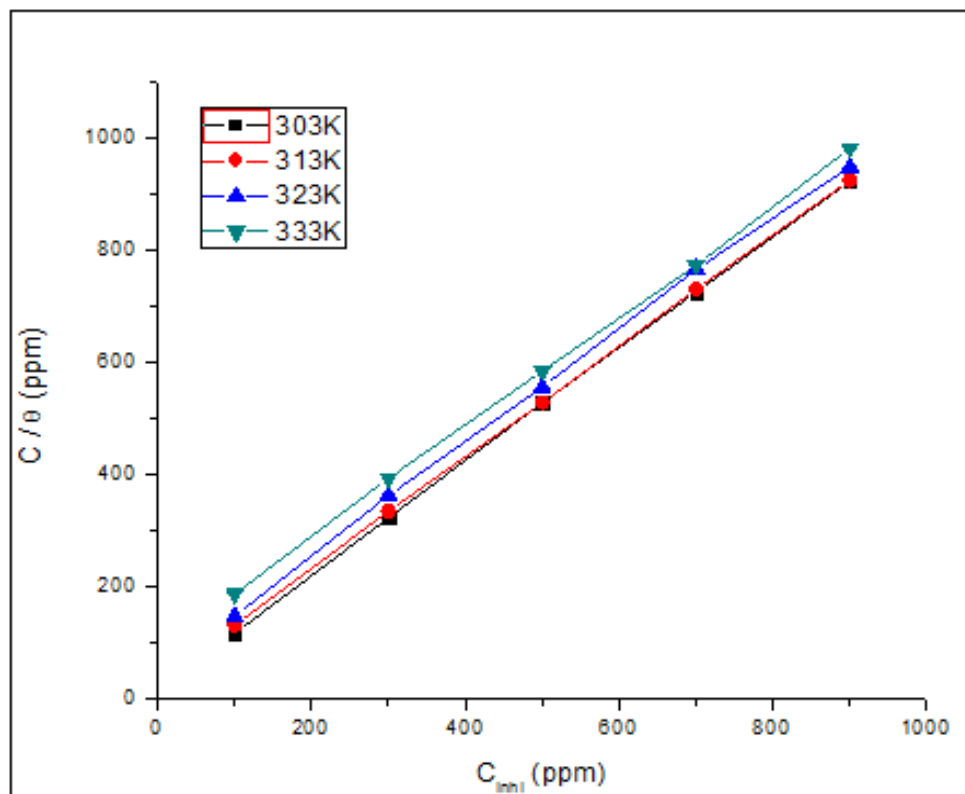


Figure 8. Langmuir plots of C/Θ Vs C_{inh} for PTC.

It is assumed that the corrosion inhibition was caused by the adsorption of PTC, and the surface coverage (θ) values of different inhibitor concentration were tested by fitting to various isotherm including Frankin, Langmuir, Temkin and Frenlich were tested in order to obtain more information about the interaction between the inhibitor molecules and the metal surface and it is observed that the linear regression between C / θ and C_{inh} , calculated by Langmuir adsorption isotherm on the metal surface, forming a strong protective barrier film which prevented the direct and indirect contact of the metal containing acid by far the test fit was obtained with the Langmuir isotherm[26, 27] The adsorption of inhibitor molecules on the corroding surfaces generally does not reach the real equilibrium and tends to a steady state. It is therefore reasonable to consider quasi equilibrium adsorption in thermodynamic by using appropriate adsorption theorem.

3.2.2 Polarization measurement

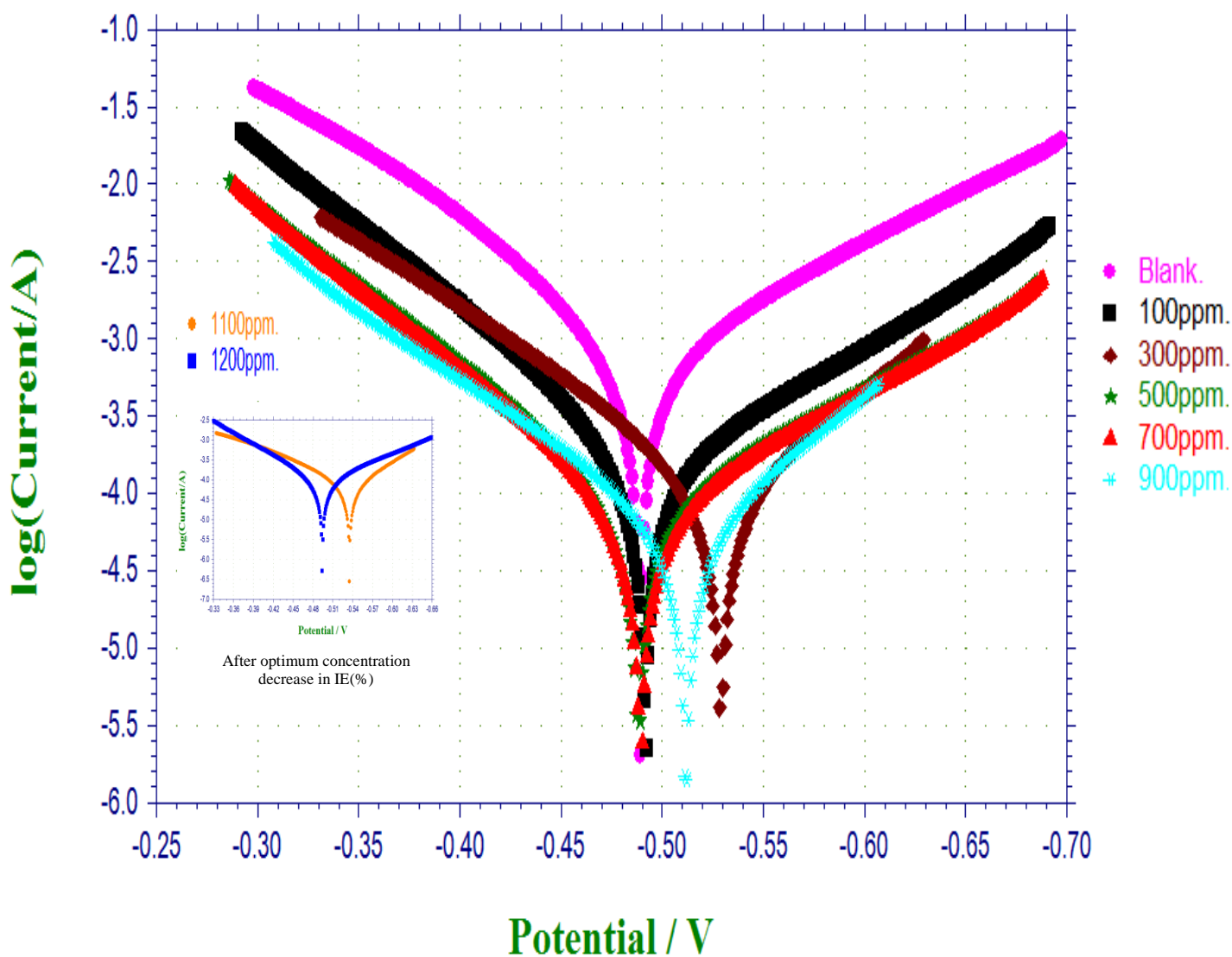


Figure 9. Potentiodynamic polarisation curves for mild steel in 1M HCl with PTC.

Table 8. corrosion parameters of mild steel in 1M HCl with PTC by polarization method.

concentration of PTC(ppm)	E _{corr} (V/SCE)	ba (mV dec ⁻¹)	bc (mV dec ⁻¹)	I _{corr} (mA/cm ⁻²)	Inhibition efficiency(%)
Blank	-489	100	73	7.776	
100	-492	110	76	1.61	79.3
300	-529	93	103	1.085	86.05
500	-488	105	70	0.8983	88.45
700	-489	106	71	0.8049	89.65
900	-512	87	105	0.6089	92.17
1100	-535	73	100	0.7921	89.81
1200	-494	93	67	0.9997	87.14

The Potentiodynamic polarization curves of mild steel performed in 1M HCl in the absence and presence of different concentrations of (PTC) at 303K are presented in Fig 9. This Phenomena can be explained in terms of electrochemical reactions. Measurements of current potential values under carefully controlled conditions can yield information on corrosion rates and films, passivity, pitting tendencies and other important phenomena. The values of electrochemical parameters associated with polarization measurements, such as corrosion potential (E_{corr}), corrosion current density (I_{corr}), Anodic (ba) and cathodic (bc) are listed in table 8. Potentiodynamic anodic polarization is the characterization of a metal specimen by its current potential relationship. The specimen potential is scanned in the positive going direction. Similarly, In potentiodynamic cathodic polarization the specimen potential is scanned in negative going direction. It suggests that the addition of inhibitor reduces anodic dissolution and the hydrogen evolution reaction [19,22]. The lower current density (I_{corr}) values in the presence of inhibitor without causing significant changes in corrosion potential (E_{corr}) suggest that the compounds are mixed type inhibitor and are adsorbed on the surface there by blocking the corrosion reaction. This reinforces the suggestion that the compounds are mixed type inhibitor.

The result indicates that the I_{corr} decreased proportionally with increase in inhibitor concentration, signifying the decrease in solubility of the metal in the solution [28]. This value was calculated from the intersection of anodic and cathodic Tafel lines of the polarization curve at E_{corr}. The maximum inhibition efficiency of the PTC inhibitor was found to be 92.17% in 1M HCl for 900ppm inhibitor concentration. Inhibition efficiency obtained from the polarization method is good agreement with inhibition efficiency obtained from the weight loss method.

3.2.3 Electrochemical Impedance Spectroscopic studies (EIS)

Electrochemical impedance spectroscopy is a special case among electrochemical techniques. Hence EIS is a small significant technique, where the analyses of the impedance spectra are a linear current voltage relation is assumed. Protective inhibitor adsorption on the metal surface causes a significant increase in impedance of the corrosion system, thus causing an increase in the resistance to the charge transfer process. The EIS experiments of PTC were carried out in order to study

corrosion behavior of PTC in more details. Fig.10A gives a clear detail of the Nyquist plots for mild steel in 1M HCl solution with and without various concentration of PTC.

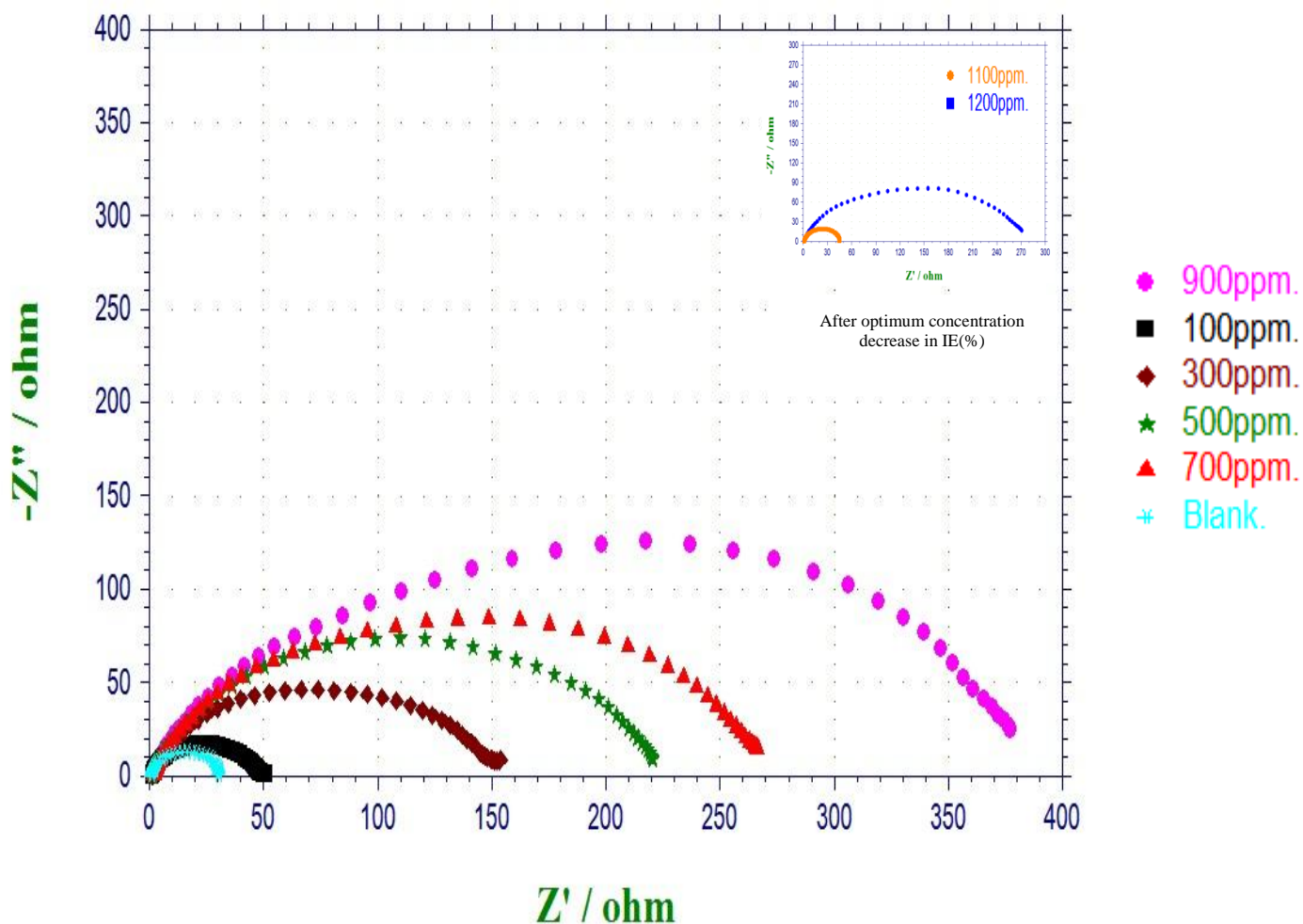


Figure 10A. Nyquist plots for mild steel in 1M HCl with PTC.

The original experimental data are represented by the symbols and the solid lines are the fitted curves based on the electrical equivalent circuit as shown in Fig.10B. [29]. Impedance parameters derived from Nyquist plots are given in Table 9. The element charge transfer resistance (R_{ct}) increased with increase in concentration of inhibitor. On the contrary, the value of double layer capacitance (C_{dl}) decreased with increase in inhibitor concentration. moreover, the radius of semicircle increases with increasing concentration of PTC. As a consequence, the obtained data shows that the corrosion of mild steel obviously inhibited in the presence of the inhibitor.

The corresponding impedance quantitative parameters are given in Table 9. The inhibition efficiency of PTC can be calculated using the below formula [30].

$$IE\% = \frac{R_{ct(inh)} - R_{ct(b)}}{R_{ct(inh)}} \times 100 \quad (7)$$

Where $R_{ct(inh)}$ and $R_{ct(b)}$ are the charge-transfer resistance with and without inhibitor for mild steel in 1M HCl, respectively.

The maximum inhibition efficiency was found to be 92.35% in 1M HCl for 900ppm PTC. From As impedance diagram for solutions examined have almost a semicircular appearance, it indicates that the corrosion of mild steel is mainly controlled by a charge transfer process. Inhibition efficiency obtained from AC impedance method is in good agreement with polarization and weight loss studies.

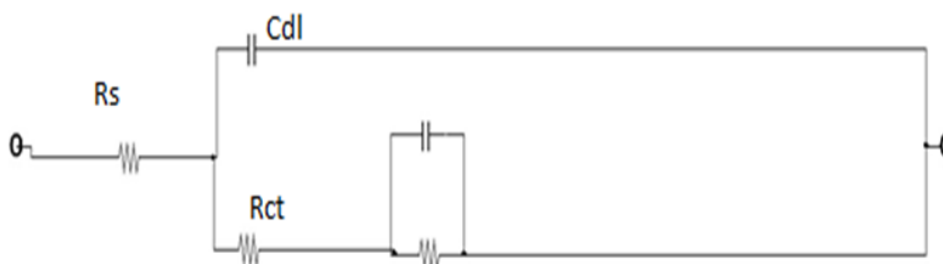


Figure 10B. Equivalent circuit diagram

Table 9. Ac impedance parameters for corrosion of mild steel in 1M HCl with PTC at 303K.

concentration of PTC(ppm)	R_{ct} (Ωcm^2)	C_{dl} ($\mu\text{F}/\text{cm}^2$)	Inhibition efficiency(%)
Blank	28.8	439.1	
100	51.01	247.9	43.54
300	152.69	82.8	81.14
500	219.82	57.5	86.9
700	264.93	47.7	89.13
900	376.32	33.6	92.35
1100	269.81	46.9	89.32
1200	43.43	291.2	33.68

3.3 Surface Analyses

3.3.1 Scanning Electron Microscopy (SEM) Analyses

SEM analysis was performed to investigate the surface morphology of the mild steel after immersion in 1M HCl in the absence and presence of 900ppm PTC for 3 hr at 30⁰C, The SEM micrograph of the deteriorated specimen in the presence of 1M HCl solution are shown in Fig(11A).

The amputating seen in the figure were result of pits formed due to exposure of mild steel to acid. The influence of the inhibitor addition(900ppm) on the mild steel in 1M HCl solution. The faceting observed in the Figure (11B) disappeared and the surface was smooth and free from pits [31]. This evident that corrosion rate is reduced by the adsorption of inhibitor molecule on the metal surface as a preservative/ protecting layer.

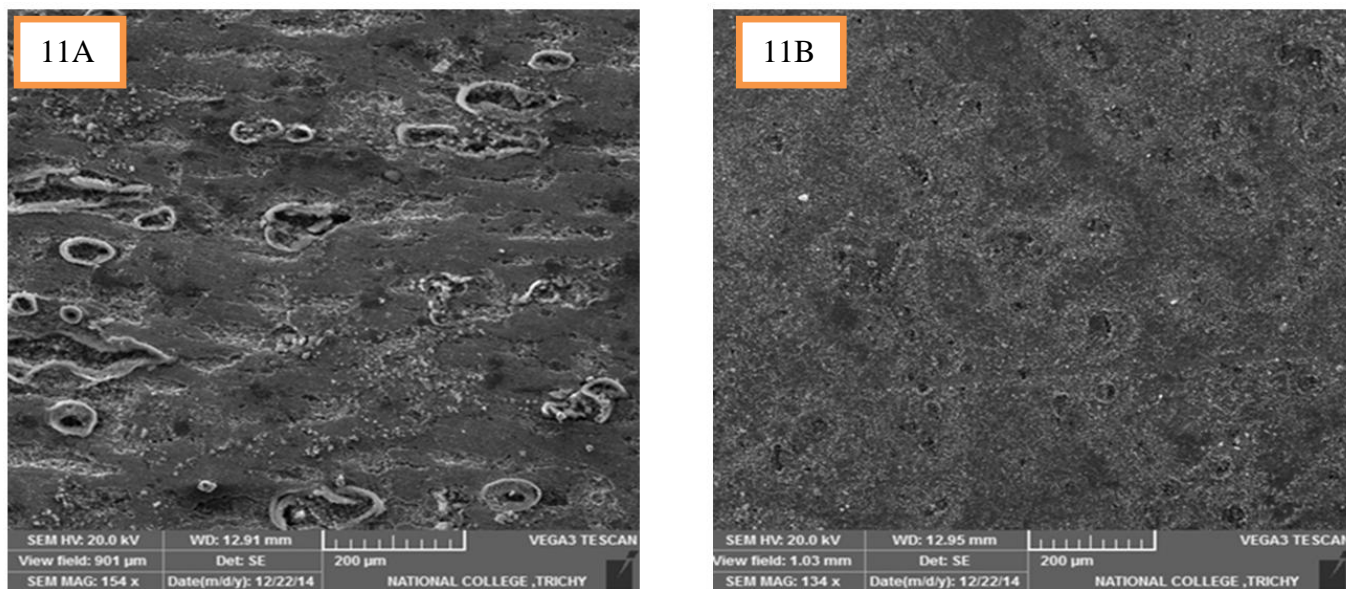


Figure 11A. SEM micrograph of mild steel surface in 1M HCl without inhibitor. **B.** SEM micrograph of mild steel surface in 1M HCl with inhibitor.

3.3.2 FT-IR Analyses.

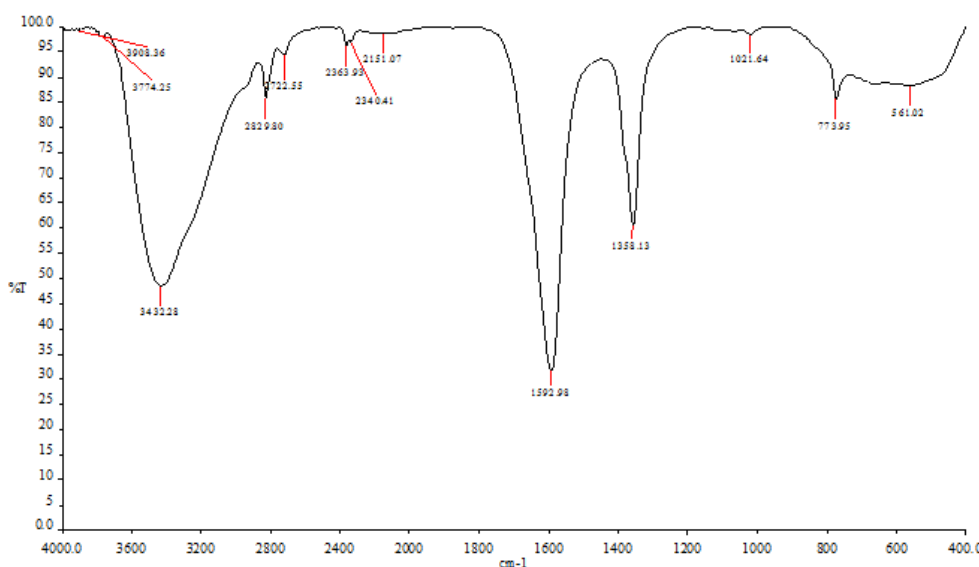


Figure 12A. FT-IR spectrum of mild steel in 1M HCl without PTC.

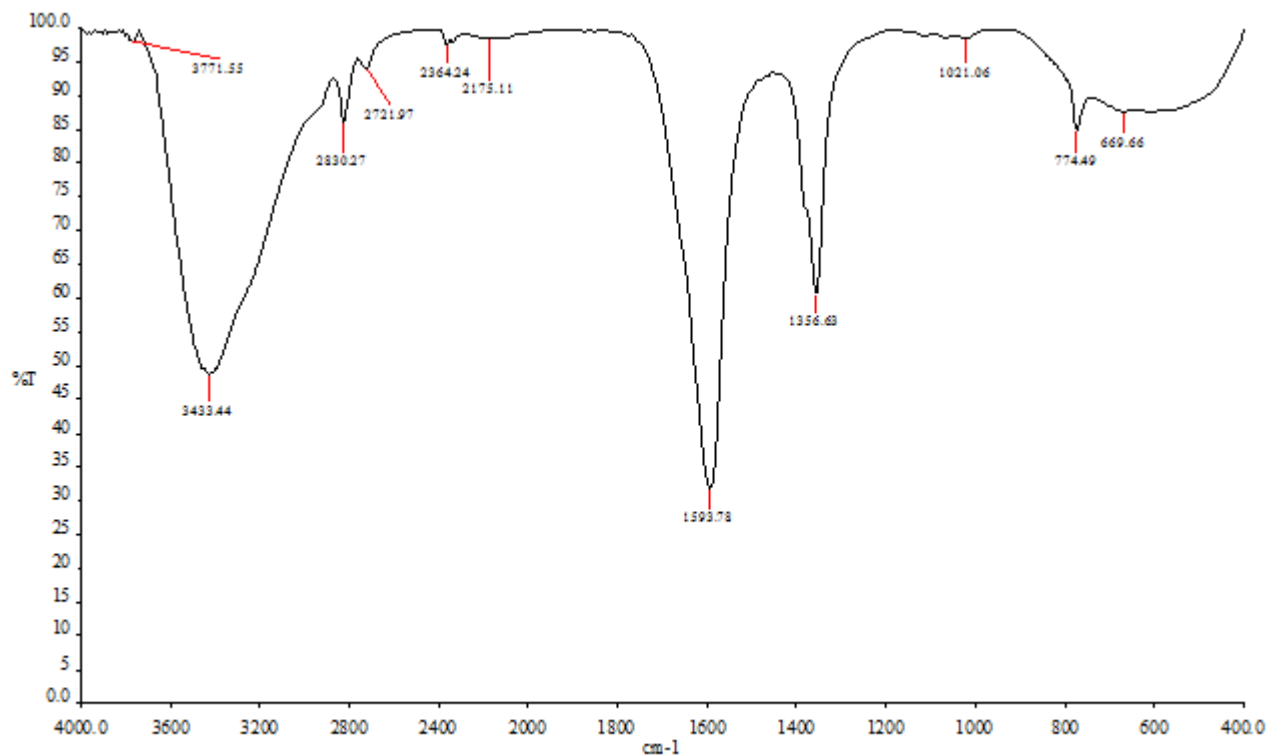


Figure 12B. FT-IR spectrum of mild steel in 1M HCl with PTC.

Table 10. FT-IR peak values of PTC for mild steel in 1M HCl

S.No	Mild steel in 1M HCl (cm ⁻¹)	4-(pyridin-2yl)-N-p-tolylpiperazine-1-carboxamide (cm ⁻¹)	Mild steel in 1M HCl with inhibitor (cm ⁻¹)	Possible groups
1	3432.28	-	-	OH
2	-	3778.16	3771.55	2 ^o Amine
3	-	3347.11	3433.44	OH (H-bonded)
4	-	3028.85	-	C-H group in aromatic ring
5	-	2857.19	2830.27	C-H Symmetric stretch
6	1592.98	-	-	δHOH
7	-	1595.56	1593.78	C=O group in the aromatic ring
8	-	1385.56	1356.63	C-H bending
9	-	1052.3	1021.06	cyclohexan ring vibration
10	561.02	-	-	γFeO
11	-	628.49	699.66	N-H Amine wag

Table 10 shows FT-IR peak values of PTC and Fig12A and 12B show the FT-IR spectra mild steel in 1M HCl with and without PTC. The peak appeared in the region of 3778.16 cm^{-1} , 2857.19 cm^{-1} , 1595.56 cm^{-1} , 1385.56 cm^{-1} , 628.49 cm^{-1} were shifted to 3771.55 cm^{-1} , 2830.27 cm^{-1} , 1593.78 cm^{-1} , 1356.63 cm^{-1} , 699.66 cm^{-1} . This is due to the interaction of oxygen, nitrogen atoms present in PTC with Fe in mild steel thereby Fe- PTC complex was formed. It reduces the corrosion mechanism [32].

4. CONCLUSION

The following conclusion were made from the study:

1. The synthesized 4-(pyridin-2yl)-N-p-tolylpiperazine-1-carboxamide(PTC) showed good inhibition efficiency for the corrosion of mild steel in 1M HCl solution and the inhibition efficiency increased with increase in the concentration of inhibitor and decreased with temperature.
2. The maximum inhibition efficiency observed in weight loss method was 98.45% in 1M HCl for PTC at 303K.
3. The optimum inhibition efficiency was achieved at the concentration of 900ppm for all the studies.
4. The negative value of ΔG_{ads} indicated that the adsorption is spontaneous and physical adsorption.
5. The adsorption of this inhibitor followed Langmuir adsorption isotherm.
6. Potentiodynamic polarization studies suggest that the inhibitor are mixed type nature.
7. EIS measurements show that charge transfer resistance(R_{ct}) increase and double layer capacitance (C_{dl}) decrease in the presence of inhibitors which suggests the adsorption of the inhibitor molecule on the surface of mild steel.
8. The SEM proves the formation of a protective film of the inhibitor.
9. FT-IR analysis of the surface film indicates the formation of Fe-PTC complex which retards the corrosion process.

References

1. I.A. Zaafarany, *Int. J. Electrochem.Sci.*, 8 (2013) 9531-9542
2. M..Bozorg, T.Shahrabi Farahani, Gh.Mohammadi Ziarani, J.Neshati,Z.Chaghazardi, P.Gholamzade and F.Ektefa, *J.Adva. mater. process.*, 2(2014) 27-38.
3. E. M. Sherif and S. Park, *Electrochim. Acta.*, 51(2006) 6556-6562.
4. Abdul Amir H. Kadhum , Abu Bakar Mohamad , Leiqaa A. Hammed , Ahmed A. Al-Amiery , Ng Hooi San and AhmedY.Musa, *NewCoumarin. Materials.*, 7(2014) 4335-4348. :doi:10.3390/ma7064335
5. K.F.Khaled, *Int. J. Electrochem., Sci.*, 3 (2008) 462-475.
6. M.J.Bahrami, S.M.A. Hosseine, and P. Pilvor, *Corros.Sci.*, 52(2010) 2793-2803
7. R.Saratha and R.Meenakshi, *Rasayan , J. Chem .*, 4(2) (2011) 251-263.
8. I. B. Obot, S.A.Umoren, and N.O.Obi-Egbedi, *J. Mater. Environ. Sci.*, 2 (2011) 49.
9. A. Ghazoui, N. Bencat, S. S.Al-Deyab, A. Zarrouk, B. Hammouti, M.Ramdani and M. Guenbour, *Int. J. Electrochem. Sci.*, 8 (2013) 2272.

10. A.H.Al Hamzi, H.Zarrok, A Zarrouk, R.Salghi, B.Hammouti, S.S.Al-Deyab, M.Bouachrine, A.Amine and F. Guenoun, *Int. J. Electrochem. Sci.*, 8 (2013)2586.
11. A.Zarrouk, M.Messali, M.R.Aouad, M.Assouag, H.Zarrok, R.Salghi, B.Hammouti and A. Chetouani, *J. Chem. Pharm. Res.*, 4(2012) 3427.
12. M. Elbakri, R. Tourir, M. Ebn Touhami, A. Zarrouk, Y. Aouine, M. Sfaira, M. Bouachrine, A. Alami and A. El Hallaoui, *Res. Chem. Intermed.*, 2012 DOI: 10.1007/s11164-012-0768-6.
13. H. Zarrok, A. Zarrouk, R. Salghi, Y. Ramli, B. Hammouti, S. S. Al-Deyab, E. M. Essassi and H. Oudda, *Int. J. Electrochem. Sci.*, 7 (2012) 8958.
14. S. John and A. Joseph, *Mater. Chem. Phys.*, 133(2012)1083-1091.
15. Y.Yan, W.Li, L.Cai and B. Hou, *Electrochim. Acta.*, 53(2008)5953-5960.
16. L. Messaadia, O. ID El mouden, A. Anejjar, M Messal, R.Salghi, O. Benali, O. Cherkaoui and A.Lallam, *J. Mater. Environ. Sci.*, 6 (2) (2015) 598-606
17. D. Ben Hmamou, R. Salghi, H. Zarrok, A. Zarrouk, B. Hammouti, M. El Hezzat and M. Bouachrin, *Adva. Mate. Corros.*, 2 (2012) 36-42
18. S.S Abd El Rehim, S.M. Sayyah and R.E. Azooz, *Portugaliae Electrochimica Acta.*, 30(1) (2012) 67-80
19. Ashish Kumar Singh, Sudhish Kumar Shukla and Eno E. Ebenso, *Int. J. Electrochem. Sci.*, 6 (2011) 5689 - 5700
20. I.Dehri and M.Ozcan, *Mater. Chem.Phys.*, 98, (2006)316-323.
21. Mahendra yadav, Sushil kumar, Indra Bahadur and Deresh Ramjugernath, *Int. J. Electrochem. Sci.*, 9(2014) 6529-6550
22. V.Hemapriya, K.Parameswari and G.Bharathy, *Rasayan .J.Chem.*, 5 (2012) 468-476
23. R.Alberty and R. Silbey, *Physical Chemistry, Second Edition.*, Wiley, New York, P.845 (1997).
24. F.W. Schapink, M. Oudeman, K.W. Leu and J.N. Helle, *Trans. Farad. Soc.*, 56(1960) 415.
25. M. Belkhaouda, L. Bammou, R. Salghi, A. Zarrouk, D. Ben Hmamou, H. Zarrok, M. Assouag, B. Hammouti and S. S. Al-Deyab, *Der.Pharmacia.letter.*, 5 (2)(2013)143-152.
26. M. Bozorg, T. Shahrabi Farahani, J. Neshati, Z. Chaghazardi and G. Mohammadi Ziarani, *Ind. Eng. Chem. Res.*, 53 (2014) 4295-4303.
27. B. Xu, W.Yang, Y. Liu, X. Yin, W. Gong and Y. Chen, *Corros. Sci.*, 78 (2014)260-268.
28. Sutiana Junaedi, Abdul Amir H. Kadhum, Ahmed A. Al-Amiery, Abu Bakar Mohamad and Mohd Sobri Takriff, *Int. J. Electrochem. Sci.*, 7 (2012)3543 - 3554
29. Yan Xie, Yuanwei Liu and Zhongnian Yang, *Int. J. Electrochem. Sci.*, 10 (2015)1292 - 1304
30. L.Elkadi, B. Mernari, M. Traisnel, F. Bentiss and M. Lagrenée, *Corros. Sci.*, 42(2000) 703.
31. V.Ramesh saliyan and Airody Vasudevan Adhikari, *Indian.J. Chem. Technol.*, 16 (2009)162-174.
32. G.Gunasekaran and L.R.Chaughan, *Corros.Sci.*, 49(2007)1143-1161.